

Adaptive strategy in multiresolution framework for uncertainty quantification

By R. Abgrall^{†‡}, P. M. Congedo^{†‡}, G. Geraci^{†‡} AND G. Iaccarino

This work illustrates a novel method to solve stochastic partial differential equations, in particular hyperbolic system of equations. Basing on the Harten multiresolution framework in the stochastic space, this method allows an adaptive refinement/derefinement in both physical and stochastic space for time dependent problems. As a consequence, an higher accuracy is obtained with a lower computational cost with respect to classical non-intrusive approaches, where the adaptivity is performed in the stochastic space only. Performances of this algorithm are tested on scalar Burgers equation and Euler system of equations, comparing with the classical Monte Carlo and Polynomial Chaos techniques.

1. Introduction

Handling uncertain operating conditions, material properties and manufacturing tolerances poses a tremendous challenge to the scientific computing community. The predictivity of the numerical simulation is strongly affected by the presence of numerous sources of uncertainty, in particular in shock-dominated flows.

The problem is to find an efficient representation of the stochastic solution, when the flow presents some discontinuities, thus producing a shock evolving in the coupled physical/stochastic space. Probabilistic uncertainty quantification (UQ) approaches represent the inputs as random variables and seek to construct a statistical characterization of few quantities of interest. Classically, among the UQ techniques, the polynomial chaos (PC) has shown its efficiency in the case of smooth responses (Le Maître & Knio (2010)). Wan and Karniadakis introduced an adaptive class of methods for solving the discontinuity issues by using local basis functions, the multi-element generalized Polynomial Chaos (ME-gPC) (Foo & Karniadakis (2010)). This strategy deals with an adaptive decomposition of the domain on which local basis are employed. In order to treat discontinuous response surfaces, Le Maître (2004*b,a*) applied a multiresolution analysis to Galerkin projection schemes. Unsteady stochastic problems have been solved by means of multi elements techniques, employing the collocation simplex method (Witteveen & Iaccarino (2012)). In all these approaches, adaptivity is applied in the stochastic space according to the regularity of the stochastic solution.

Recently, Abgrall & Congedo (2011) introduced a new class of finite volume (FV) schemes formulated in both the physical and stochastic space. This formulation allows to reach the same accuracy in both spaces employing well-known reconstruction techniques used in high-order FV schemes. This method preserves the number of equations and requires only some slight modifications to the existing deterministic solver. In a natural way is also possible to incorporate any kind of probability distribution function (pdf), even discontinuous or time dependent. In Abgrall *et al.* (2012*a,b*), a method is presented that is based on the classical MR framework of Harten extended to the stochastic space.

[†] Team Bacchus, INRIA Bordeaux–Sud-Ouest

[‡] Institute de Mathematiques de Bordeaux, University of Bordeaux

Here, the aim is to build a numerical method for solving efficiently sPDE, that is obtained by reducing the number of points employed in the physical/stochastic space by means of an adaptive technique. The present work is focused on the extension of Abgrall *et al.* (2012a) to deal with spatial dependent solutions. The focus of this research is on non-linear hyperbolic systems with discontinuous solutions in both physical and stochastic spaces. Two different test cases are considered: the scalar Burgers equation and the Euler system of equations, in particular the simulation of a perfect gas flow in a shock-tube configuration.

The paper is organized as follows. In section §2, motivation for a new technique for UQ is illustrated. The section §3 introduces briefly the Truncate and Encode (TE) strategy in the stochastic space and in section §3.3 the extension of the method to spatial and time dependent solution is presented. Numerical results are presented in the section §4. Some conclusions and perspectives are drawn in section §5.

2. Motivation

In this section, we want to illustrate the different perspective driving us in the context of stochastic PDE.

Let us start by considering a differential operator \mathcal{L} applied to a function u that is dependent on the space \mathbf{x} (defined as $\mathbf{x} \in D \subset \mathbf{R}^n$), on the time $t \in [0, T]$ and on a vector of random parameters $\boldsymbol{\xi} \in \Xi \subset \mathbf{R}^d$ (associated to the probability distribution $p(\boldsymbol{\xi}) = \prod_{i=1}^d p_i(\boldsymbol{\xi}_i) > 0$):

$$\mathcal{L}(u(\mathbf{x}, t, \boldsymbol{\xi})) = 0, \quad (2.1)$$

with specific initial and boundary conditions.

The aim of the UQ is to compute statistical moments of u , such as for example expectancy $\mu(\mathbf{x}, t; u)$ and variance $\text{Var}(\mathbf{x}, t; u)$, defined as follows

$$\begin{aligned} \mu(\mathbf{x}, t; u) &= \int_{\Xi} u(\mathbf{x}, t, \boldsymbol{\xi}) p(\boldsymbol{\xi}) d\boldsymbol{\xi} \\ \text{Var}(\mathbf{x}, t; u) &= \int_{\Xi} (u(\mathbf{x}, t, \boldsymbol{\xi}) - \mu(\mathbf{x}, t; u))^2 p(\boldsymbol{\xi}) d\boldsymbol{\xi}. \end{aligned} \quad (2.2)$$

Computing efficiently statistics ((2.2)) for each position in the physical (\mathbf{x}) and time (t) spaces is very challenging when u is discontinuous. This is a very common problem in compressible fluid-dynamics where a shock generated in the flow can propagate in the coupled physical/stochastic space. In this case, this translates mathematically in solving a non-linear hyperbolic system of equations in presence of a discontinuity.

Classically this problem can be solved by using non-intrusive techniques, based for example on PC or collocation approaches. These techniques share two fundamental steps: i) solving N_{ξ} times (2.1) for a specific set of samplings $\{\boldsymbol{\xi}_i\}_{i=1}^{N_{\xi}}$, ii) using the ensemble of solutions $u_i(\mathbf{x}, t, \boldsymbol{\xi}_i)$ for computing an approximation of statistics (2.2). Finally, the global numerical cost associated to solve (2.2) is equal to $N = N_x \times N_t \times N_{\xi}$, where N_x , N_{ξ} and N_t are the number of points in the physical, stochastic and time spaces, respectively. This can lead to a dramatic increase of the computational cost: if in a specific location \mathbf{x} , a high-gradient or a discontinuity exist, more samplings in the stochastic space should be considered for computing statistics (2.2), and then solving (2.1) for each adding sampling is mandatory. On the contrary, remark that if there is a discontinuity in the stochastic space only (thus not propagating in the physical space), such as for example a jump in

the pdf, an adaptive non-intrusive method could be capable to solve the problem with a reduced computational cost.

Finally, when using non-intrusive approaches, it is not possible to locally refine/derefine the stochastic mesh following how the solution evolves in space and time. This could require an high number of points N_ξ when solving problems with high-gradients or even discontinuities evolving in the coupled physical/stochastic space and in time.

The aim of this work is to build an intrusive numerical schemes able to refine/derefine the stochastic mesh during the time, *i.e.* the number of points in the stochastic space becomes a function of space and time ($N_\xi = N_\xi(\mathbf{x}, t)$). A detailed description of this algorithm is given in the next sections.

In this work, we introduce a global error estimation including the variation of the solution in space and time. Then, the error norms associated to a given statistical moment, *i.e.* μ^m , are computed in $D \times T \times \Xi$ space as follows (here explicitly for $n = d = 1$)

$$\begin{aligned} \text{err}_{\mu^m}|_{L_p} &= \left(\frac{1}{N_t \times N_x} \sum_{i=1}^{N_t} \sum_{j=1}^{N_x} |\mu^m(x_j, t_i; u) - \mu_{ref}^m(x_j, t_i; u)|^p \right)^{\frac{1}{p}} \\ \text{err}_{\mu^m}|_{L_\infty} &= \max_{\substack{i=1 \dots N_t \\ j=1 \dots N_x}} |\mu^m(x_j, t_i; u) - \mu_{ref}^m(x_j, t_i; u)|, \end{aligned} \quad (2.3)$$

where μ_{ref}^m is the reference solution (that is computed systematically in this paper by means of a Monte Carlo method).

These norms are different from what is usually done in literature, where the error norms are computed at some specific spatial location or they are computed for some quantity of interest not dependent on the space \mathbf{x} .

3. A spatial Truncate and Encode strategy

In this section, we present the spatial Truncate and Encode (TE) algorithm. First, we define the main operator used in the classical MultiResolution framework. Secondly, the TE strategy is illustrated on a simple scalar function dependent only on the stochastic variable. Finally the extension to a space-dependent function is considered, *i.e.* the spatial TE strategy, and an example is given on the Burgers equation.

3.1. Operators in classical MR framework

Let us consider a scalar function $u = u(\xi)$ defined in the stochastic space with $\Xi = [0, 1]$. We indicate the generic mesh level k of N_k equally spaced intervals of length h_k as

$$\mathcal{G}^k = \{\xi_j^k\}_{j=0}^{N_k}, \quad \xi_j^k = jh_k, \quad h_k = 2^k h_0, \quad N_k = N_0/2^k.$$

In the classical point-value setting of the Harten framework (see for instance Arandiga *et al.* (2009)), the solution is assumed to be known at the finest level (N_0). This assumption allows to obtain a representation of the solution on the nested sequence of meshes \mathcal{G}^k with $k = 0, \dots, L$ where L is the coarsest level (called as *encoding* procedure). Once the nested representation of the function is obtained, a criterion is introduced to compress the solution and only the significative points are retained. This leads to the so-called *truncation* procedure. At the end of the two steps of *encoding* and *truncation*, the solution can be represented with its multiresolution structure. At each time step, the finest level can be reconstructed from the coarsest one (the so-called *decoding* procedure). Main operators of MR Harten framework are the following:

• **Encoding:** the solution represented on the finest mesh \mathcal{G}^0 is employed to obtain a hierarchical representation on a nested sequence of levels $k = 1, \dots, L$ where \mathcal{G}^k are obtained directly from \mathcal{G}^{k-1} without considering the odd points. For each *missing point* $\xi_j^k \in \mathcal{G}^{k+1} - \mathcal{G}^k$, a *detail* or *wavelet* is computed as $d_j^k = u_{2j-1}^{k-1} - \tilde{u}_{2j-1}^{k-1}$, where \tilde{u}_{2j-1}^{k-1} is an approximation of the value employing a whatever interpolation operator $\mathcal{I}(\xi; u^k)$ that interpolates the function u on the level k in the point ξ . In the present work, we considered a linear interpolation operator. However, the extension to more complex and accurate interpolation would lead to similar algorithms (see Arandiga et al. (2009)). The final result of the *encoding* procedure is to obtain a multiresolution u_M representation of u : $(u_M)^T = (d^1, d^2, \dots, d^L, u^L)$ where $d^k = \{d_j^k\}$ and $k = L$ is the coarsest level. For brevity, the procedure can be re-arranged in matrix form: $u_M = Mu^0$.

• **Truncation:** in order to obtain a data compression of the solution at the finest level \hat{u}^0 , a threshold can be introduced to eliminate the non-significant *wavelets*. In particular, a truncated *detail* is defined as follows

$$\hat{d}_j^k = \begin{cases} d_j^k & \text{if } |d_j^k| > \varepsilon_k \\ 0 & \text{if } |d_j^k| \leq \varepsilon_k. \end{cases} \quad (3.1)$$

As a consequence, the truncated multiresolution representation consists in $\hat{u}_M = (\hat{d}^1, \hat{d}^2, \dots, \hat{d}^L, u^L)$.

• **Decoding:** once the truncation is performed, the solution on the finest level can be obtained directly from the coarsest one, *i.e.* $\hat{u}^0 = M^{-1}\hat{u}_M$. The following estimation holds (see Harten (1994) for a proof)

$$\|u^0 - \hat{u}^0\| \leq C\varepsilon, \quad \text{if } \varepsilon_k = \varepsilon/2. \quad (3.2)$$

3.2. TE strategy

After some definitions given in the previous paragraph, we can now introduce the TE strategy, that permits to perform both the encoding and truncation procedures starting from the coarsest level to the finest. The TE strategy is constituted by the following steps (the notation is the same of the Harten's multiresolution framework, *i.e.* $k = 0$ for the finest level and $k = L$ for the coarsest):

- Preliminary operations
 - Fix a threshold ε
 - Fix an index $m_{\max} \in \mathbf{N}$ for the maximum allowed level ($N_{\max} = N_0 = 2^{m_{\max}}$);
 - Fix an index $m_L \in \mathbf{N}$ for the coarsest level ($N_L = 2^{m_L}$);
 - The condition $m_L < m_{\max}$ must be satisfied.
- Evaluation of the function u at each location of the coarsest level $u(\xi_j^L) = u_j^L$ with $j = 0, \dots, N_L$ where

$$\mathcal{G}^L = \{\xi_j^L\}_{j=0}^{N_L}, \quad \xi_j^L = jh_L, \quad h_L = 2^L h_0, \quad N_L = N_0/2^L, \quad (3.3)$$

and $h_0 = 1/N_0$. Each level can be labeled computing the equivalent index k_{eq}

$$k_{eq} = \log_2 \left(\frac{N_0}{N_{k_{eq}}} \right).$$

- Evaluation of the subsequent level, with respect to the coarsest one

$$\mathcal{G}^{L-1} = \{\xi_j^{L-1}\}_{j=0}^{N_{L-1}}, \quad \xi_j^{L-1} = jh_{L-1}, \quad h_{L-1} = 2^{L-1}h_0, \quad N_{L-1} = N_0/2^{L-1}. \quad (3.4)$$

- The adaptive strategy begins by means of the following recursive procedure
 - A - The *wavelets coefficients* are computed for the present level k as

$$d_j^k = u_j^k - \mathcal{I}(\xi_j^k; u^k) \quad \text{for } 0 \leq j \leq N_k \quad \text{with } j \text{ odd}; \quad (3.5)$$

When the linear interpolation is used, $\mathcal{I}(\xi_j^k; u^k) = \frac{1}{2} \left(u_{\frac{j+1}{2}}^{k+1} + u_{\frac{j-1}{2}}^{k+1} \right)$.

B - The wavelets coefficients are compared with the threshold $\varepsilon_k = \varepsilon/2^k$. If $|d_j^k| > \varepsilon_k$ then the two nodes ξ_{2j+1}^{k-1} and ξ_{2j-1}^{k-1} will be flagged as active on the next finer mesh \mathcal{G}^{k-1} . If $|d_j^k| < \varepsilon_k$ then the *wavelets* is truncated, i.e. its value is posed zero.

C - The new level $k-1$ is generated if $k > 0$ and the function u is evaluated only on the activated points.

D - Moving from a level k to the finer adjacent one $k-1$, three different cases are possible:

- If $\xi_j^k \in \mathcal{G}^k \cap \mathcal{G}^{k+1}$ then $u_j^k = u_{2j}^{k+1}$ (shifting)
- If $\xi_j^k \notin \mathcal{G}^k \cap \mathcal{G}^{k+1}$ and it is not flagged then interpolate

$$u_j^k = \mathcal{I}(\xi_j^k; u^k) \quad (3.6)$$

- If $\xi_j^k \notin \mathcal{G}^k \cap \mathcal{G}^{k+1}$ and it is flagged as active (from the step B of the algorithm) then evaluate, i.e. call the model applying the numerical method (efficiency of the method is increased when the number of calls is reduced).

E - The algorithm stops when the maximum level is reached or when all the *wavelets* coefficients can be truncated (at a certain level $k > 0$).

Since the aim is to compute statistics as defined in (2.2), the presented algorithm is employed on the product between the solution u and the probability distribution of the random parameter. Consequently, this allows to consider a whatever form of the pdf even discontinuous and time dependent without loss of information.

3.3. Extension to spatial and time dependent problems

Here, we extend the TE algorithm for including a physical space and time dependences of the solution, thus leading to the spatial-TE (sTE) strategy. As a consequence, let us consider $u = u(\xi, \mathbf{x}, t)$, and a given discretization in the physical space and time. We employ the notation $u_i^n(\xi)$ to represent the function $u(x_i, t_n, \xi)$. Using this form, at a fixed time t_n and at a fixed spatial location x_i , the function u reduces to depend only on the stochastic space ξ , as already done in the previous section.

The sTE algorithm starts with the same preliminary operations of the standard TE method: a threshold ε , a minimum m_l and a maximum m_{max} level are fixed. The initial condition is analytically evaluated on the finest mesh

$$u_{ij}^0 = u(x_i, 0, \xi_j) \quad \forall \quad i = 0, \dots, N_x - 1 \quad \text{and} \quad j = 0, \dots, N_0. \quad (3.7)$$

Then, a recursive algorithm is applied at each time step: for each spatial location x_i with $i = 0, \dots, N_x - 1$, the standard TE algorithm described in the previous section is applied to the function dependent only from the stochastic space $u(x_i, t_n, \xi)$ obtaining a multiresolution representation for each spatial location x_i . Before passing to the next iteration in time, the solution on the whole space at time t_n , $u(x, t_n, \xi)$, is known. Finally, the procedure can be repeated for each time step until reaching the final time T .

According to the regularity of the function $u(x, t, \xi)$, the multiresolution representation can change from a spatial location to another one, *i.e.* different locations of the significative points and different maximum level that are reached, can be found. Remark that, in high-regularity region, the sTE could stop before reaching the maximum level (see §3).

3.4. Application to Burgers equation

In this section, we apply the sTE algorithm to the 1D inviscid Burgers equation, defined as follows

$$\begin{cases} \frac{\partial u(x, t, \xi)}{\partial t} + \frac{\partial f(u(x, t, \xi))}{\partial x} = 0 & \text{for } x \in [0, 1] \\ u(x, 0, \xi) = u_0(x, \xi), \end{cases} \quad (3.8)$$

defined for $t \in [0, T]$ with flux $f(u(x, t, \xi)) = \frac{1}{2}u^2(x, t, \xi)$ and with one uncertainty on the initial condition $u_0(x, \xi)$ and periodic boundary conditions. We suppose in the following to employ, without loss of generality, the normalized stochastic parameters $\xi = [0, 1]$.

Using a spatial discretization with N_c equally spaced points $x_i = i\Delta x$ for $i = 0, \dots, N_c - 1$ and $\Delta x = 1/(N_c - 1)$, a classical finite volume (FV) Godunov scheme and a forward Euler formula in time ($t_n = n\Delta t$ with $n = 1, \dots, N_t$ and $\Delta t = 1/N_t$) (see LeVeque (1992) for more details) are applied to (3.8) as follows

$$u_i^{n+1}(\xi) = u_i^n(\xi) + \frac{\Delta t}{\Delta x} \left(F_i^n(u_{i-1/2}^n(\xi)) - F_i^n(u_{i+1/2}^n(\xi)) \right) \quad \forall \xi \in [0, 1], \quad (3.9)$$

where $F_i^n(u_{i-1/2}^n(\xi))$ is a consistent numerical flux. In this work, we employed an exact Riemann solver in order to obtain the flux at the interfaces $x_{i-1/2} = x_i - \frac{1}{2}\Delta x$ and $x_{i+1/2} = x_i + \frac{1}{2}\Delta x$ of cell surrounding the node x_i .

Let us now apply the sTE strategy. We discretize the equation in the stochastic space employing as initial condition the analytical discretization (3.7) on the finest stochastic mesh \mathcal{G}^0 associated to the maximum level m_{max} , thus obtaining

$$u_{ij}^{n+1} = u_{ij}^n - \frac{\Delta t}{\Delta x} \left(F_{ij}^n(u_{i+1/2}^n(\xi_j)) - F_{ij}^n(u_{i-1/2}^n(\xi_j)) \right), \quad (3.10)$$

where the pedix j refers to the stochastic space $u_{ij}^n = u(x_i, t_n, \xi_j)$ and the numerical flux is equal to $F_{ij}^n(u_{i-1/2}^n) = \frac{1}{2}u^2(x_{i-1/2}, t_n, \xi_j)$.

First, remark that the solution is time dependent, then at each time step the function, in case of evaluation, must employ the information from the previous time step. Secondly, remark that using (3.10), in order to advance the solution in time at the physical location x_i , fluxes $F_{ij}^n(u_{i-1/2}^n(\xi_j))$ and $F_{ij}^n(u_{i+1/2}^n(\xi_j))$ should be computed. Using the exact Riemann solver (see LeVeque (1992)) to compute the fluxes at the interface, solutions at the neighbor nodes x_{i-1} and x_{i+1} are then needed: $F_{ij}^n(u_{i-1/2}^n(\xi_j)) = F_{ij}^n(u_{i-1/2}^n(\xi_j))(u_{i-1}^n(\xi_j), u_i^n(\xi_j))$ and $F_{ij}^n(u_{i+1/2}^n(\xi_j)) = F_{ij}^n(u_{i+1/2}^n(\xi_j))(u_i^n(\xi_j), u_{i+1}^n(\xi_j))$. If, for instance, the solution at the node x_{i-1} is not available, should be reconstructed. This can be done employing the interpolation operator on the proper stencil along the stochastic space:

$$u(x_{i-1}, t_n, \xi_j) = \mathcal{I}(\xi_j; u_{i-1}^n(\xi)). \quad (3.11)$$

For example, if the *missing point* ξ_j is surrounded by two points ξ_{j-1} and ξ_{j+1} of the finer stochastic mesh, in the case of linear interpolation, the stencil is constituted by the two neighbors ξ_{j-1} and ξ_{j+1} :

$$u(x_{i-1}, t_n, \xi_j) = \frac{1}{2}(u(x_{i-1}, t_n, \xi_{j-1}) + u(x_{i-1}, t_n, \xi_{j+1})). \quad (3.12)$$

Case	N_x	N_t	Δt	ν
A	101	1500	8×10^{-3}	0.0
B	101	1750	7×10^{-3}	0.01
C	201	6000	2×10^{-3}	0.0
D	201	6050	2×10^{-3}	0.01

TABLE 1. Cases presented.

This section presented the extension of the TE strategy to spatial and time dependent problem. Results obtained using this sTE method on Burgers and Euler equations are presented in the next section.

4. Numerical results

Concerning all the results presented in this section, the error norms are computed systematically with respect to the fully converged MC solution with $N_\xi = 2 \times 10^6$. The error norms for mean and variance are computed in L_1 , L_2 and L_∞ spaces. Moreover, the errors are compared with the so-called non compressed solution, where a trapezoidal rule quadrature technique between equally spaced points is taken into account.

4.1. Burgers equation

The Burgers equation and the viscous version are solved taking into account one uncertainty in the initial condition. It is defined as follows

$$\begin{cases} \frac{\partial u(x, t, \xi)}{\partial t} + \frac{\partial \frac{1}{2} u^2(x, t, \xi)}{\partial x} = \nu \frac{\partial^2 u(x, t, \xi)}{\partial x^2} & \text{for } x \in D \text{ and } t \in [0, T] \\ u(x, 0, \xi) = u_0(x, \xi), \end{cases} \quad (4.1)$$

where the viscous term on the right side disappears in the case of the inviscid Burgers equation. Periodic boundary conditions are applied in both cases. We employed a FV Godunov scheme, *i.e.* piecewise constant approximation on each cell, with a central second order discretization for the viscous term when considered. The fluxes at the interfaces are computed employing an exact Riemann solver. Two initial conditions are taken into account, both continuous and discontinuous.

The discontinuous initial case is solved using $x \in [-1, 1]$ and $\xi \in [-\frac{1}{2}, \frac{1}{2}]$. Different settings are considered resumed in Table 1. The following initial condition is considered

$$u^0(x, \xi) = \begin{cases} 1 & \text{if } \xi \leq x \leq \xi + \frac{1}{2}, \\ 0 & \text{otherwise.} \end{cases} \quad (4.2)$$

Moreover, the continuous case is solved with $x \in [0, 1]$, $\xi \in [\frac{3}{2}, \frac{5}{2}]$, $N_x = 101$ and $N_t = 1300$ with $\Delta t = 4 \times 10^{-3}$. The initial condition employed is defined as $u^0(x, \xi) = \sin(x\xi\pi)$.

Let us focus on the case A. We report the error norms for the variance in figure 1. The error is plotted versus the total number of points in the whole space $N = N_x \times N_t \times N_\xi$, thus considering the total cost of a simulation. Curves obtained by means of sTE displays systematically better convergence rates than MC and PC. Three different curves are computed by means of the sTE strategy: they differ only for the initial level chosen to initialize the solution (m_i). Obviously, an higher level need an higher number of points,

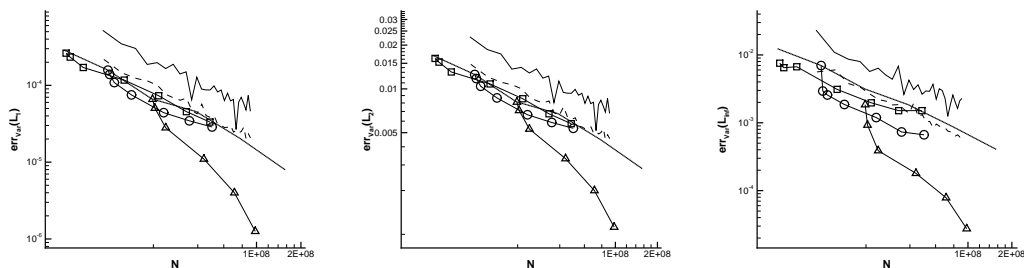


FIGURE 1. Error norms for the variance of the inviscid Burgers equation with discontinuous initial condition. L_1 , L_2 and L_∞ norms at left, middle and right respectively. MC (continuous line), PC (dashed line), sTE with $m_l = 4$ (squares), $m_l = 5$ (circles) and $m_l = 6$ (triangles). The non-compressed solution is the dotted one.

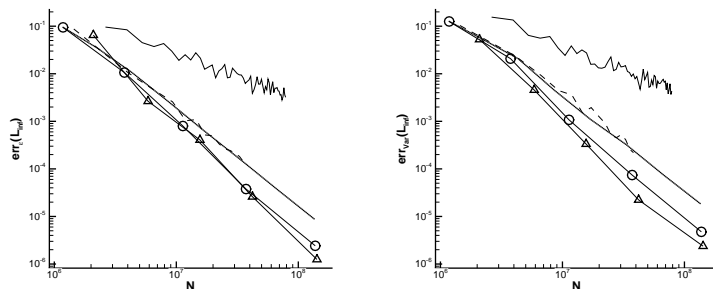


FIGURE 2. Error L_∞ norms for the mean (left) and variance (right) of the inviscid Burgers equation with continuous initial condition. MC (continuous line), PC (dashed line), sTE with $s = 2$ (circles), $s = 3$ (triangles). The non-compressed solution is the dotted one.

but as it is evident from figure 1, when the initial level is high enough to capture all the characteristics of the function, the convergence rate of the scheme increases too.

Qualitatively, same results hold for the continuous case. In figure 2, the L_∞ norms are reported for both mean and variance. Two curves generated by means of the sTE method are obtained with two different separation ratios, *i.e.* $s = m_{max} - m_l$, that represents a measure of the compressibility capability of the method. Also in this case both curves show a smoother behavior with respect to both MC and PC. Moreover, the convergence rate increases with higher separation ratio. Compression solution capabilities are remarkable, if the convergence rate is compared to the non compressed solution one.

In figure 3, two meshes in the physical/stochastic spaces are reported at the same time step ($t = 5.2$) using the non adaptive and the adaptive approach. It clearly shows how the sTE strategy automatically places more points in the high-gradients regions while the mesh is derefined in the smoother regions.

4.2. Shock-tube configuration

In this section, let us apply the sTE strategy to an Euler system of equations, in particular to the simulation of a shock-tube configuration. One uncertainty is taken into account defining the initial condition, namely the position of the diaphragm. The quasi-1D Euler equations are solved with second-order accuracy in time and space. The convective fluxes

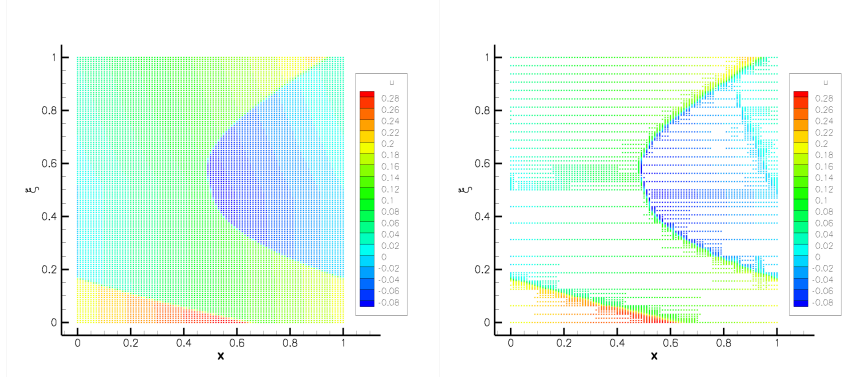


FIGURE 3. Complete (left) and compressed (right) meshes for the inviscid Burgers problem with uncertain continuous initial condition. The maximum level is fixed to $m_{max} = 12$ and the minimum level to $m_l = 2$. The threshold is $\varepsilon = 10^{-1}$.

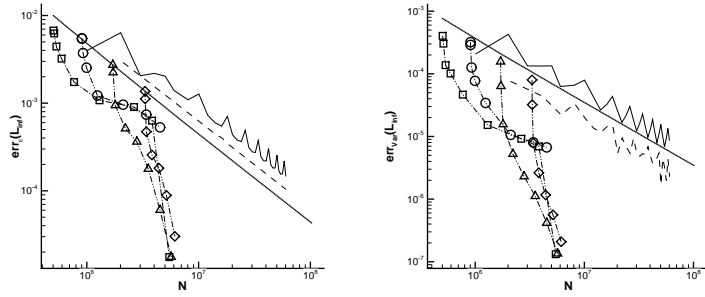


FIGURE 4. Error L_∞ norms for the mean (left) and variance (right) of the Euler system with continuous initial condition. MC (continuous line), PC (dashed line), sTE with $m_l = 1$ (squares), $m_l = 2$ (circles), $m_l = 3$ (triangles) and $m_l = 4$ (diamonds). The non-compressed solution is the dotted one.

are discretized using the Roe numerical flux and a second-order limited MUSCL variable reconstruction.

An uncertain initial condition is chosen as $(u = 0 \quad \forall x \in [0, 1])$

$$\begin{cases} \rho = 1 & \text{for } x < \xi \\ \rho = 0.125 & \text{for } x \geq \xi \end{cases} \quad (4.3)$$

The stochastic parameter is assumed to be $\xi \in [0.46, 0.5]$. The total time of the simulation is fixed to $T = 0.25$ with $N_t = 500$ equally spaced time steps of $\Delta t = 5 \times 10^{-4}$. The spatial mesh employed is constituted by $N_x = 201$ points.

In figure 4, the error norms L_∞ are reported for both mean and variance. Different curves associated to sTE method are reported. As seen for the previous inviscid Burgers case, different evolutions of the errors are obtained varying the minimum level m_l (fixed for each curve) and allowing, progressively, an higher maximum level m_{max} . The results are always better than the non-intrusive MC and PC. The non-compressed solution is also reported displaying capabilities of sTE with respect to a fixed quadrature rule.

5. Concluding remarks

This paper presents an innovative adaptive strategy for stochastic differential equations, the sTE algorithm, inspired to the classical Hartens framework. A representation of the solution on a finest grid is computed starting from a coarsest one, with a reduced number of function evaluations. As a consequence, only a reduced set of point values on the finest grid is evaluated, while the remaining set is obtained by interpolation (from the previous levels). This procedure moves recursively, with a combination of interpolation and evaluation, from the coarsest level to the finest and from each time step to the successive one. The sTE strategy is applied to the associated stochastic space obtaining the MR representation of the solution at each time step, for each spatial node, *i.e.* the representation of the stochastic function obtained at a fixed physical space and time.

The sTE strategy is applied first to the Burgers equations and then to the simulation of a shock-tube configuration. The sTE displays very promising results in terms of accuracy, convergence and regularity with respect to more classical techniques, such as MC and PC. Future work will be oriented towards the use of an high-order of interpolation.

Acknowledgments

This work was partially supported by the CTR Summer Program 2012 - Stanford. This work was partially financed by the associated team AQUARIUS (Joint team from INRIA and Stanford University). Remi Abgrall and Gianluca Geraci have been partially supported by the ERC Advanced Grant ADDECCO N. 226316.

REFERENCES

- ABGRALL, R. & CONGEDO, P. M. 2011 A semi-intrusive deterministic approach to uncertainty quantifications in non-linear fluid flow problems. *Accepted for publication in Journal of Computational Physics* .
- ABGRALL, R., CONGEDO, P. M. & GERACI, G. 2012a A One-Time Truncate and Encode Multiresolution Stochastic Framework. *Tech. Rep.*. RR-7967, INRIA.
- ABGRALL, R., CONGEDO, P. M. & GERACI, G. 2012b Toward a Unified Multiresolution Scheme in the Combined Physical/Stochastic Space for Stochastic Differential Equations. *Tech. Rep.*. RR-7996, INRIA.
- ARANDIGA, F., CHIAVASSA, G. & DONAT, R. 2009 Harten framework for multiresolution with applications. *Boletín SEMA* **31** (31), 73–108.
- FOO, J. & KARNIADAKIS, G. E. 2010 Multi-element probabilistic collocation method in high dimensions. *Journal of Computational Physics* **229**, 1536–1557.
- HARTEN, A. 1994 Adaptive multiresolution schemes for shock computations. *Journal of Computational Physics* **135** (2), 260–278.
- LE MAÎTRE, O. 2004a Multi-resolution analysis of Wiener-type uncertainty propagation schemes. *Journal of Computational Physics* **197** (2), 502–531.
- LE MAÎTRE, O. 2004b Uncertainty propagation using WienerHaar expansions. *Journal of Computational Physics* **197** (1), 28–57.
- LE MAÎTRE, O. & KNIO, O. 2010 *Spectral Methods for Uncertainty Quantification: With Applications to Computational Fluid Dynamics*. Springer Verlag.
- LEVEQUE, R. 1992 *Numerical Methods for Conservation Laws*. Birkhäuser.
- WITTEVEEN, J. A. S. & IACCARINO, G. 2012 Simplex stochastic collocation with random sampling and extrapolation for nonhypercube probability spaces. *SIAM Journal on Scientific Computing* **34**, A814–A838.